

Supporting Information

Selective Chiral Symmetry Breaking and Luminescent Sensing of Zn(II) Metal-Organic Framework

Zheng Cui, Lei Zhou, Bowen Qin, Baolei Zhou, Xiaoying Zhang,* Wenliang Li* and Jingping Zhang*

Advanced Energy Materials Research Center, Faculty of Chemistry, Northeast Normal University,
Changchun 130024, P. R. China

*E-mail: jpzhang@nenu.edu.cn, zhangxy218@nenu.edu.cn, liwl926@nenu.edu.cn

Table S1. Crystallographic data for compounds **1P** and **1M**.

Compound	1P	1M
Formula	$C_{54}H_{24}Zn_{4.5}N_{12}O_{25}$ [(CH ₃) ₂ NH ₂] ₅ [(CH ₃) ₂ NCHO] ₉ (H ₂ O) _{15.5} *	$C_{54}H_{24}Zn_{4.5}N_{12}O_{25}$ [(CH ₃) ₂ NH ₂] ₅ [(CH ₃) ₂ NCHO] ₁₀ (H ₂ O) _{17.5} *
Formula mass	2702.65	2811.78
Crystal system	Cubic	Cubic
Space group	<i>F</i> 4 ₁ 32	<i>F</i> 4 ₁ 32
<i>a</i> , Å	45.1476(7)	45.1207(6)
<i>V</i> , Å ³	92025(4)	91860(4)
Temperature, K	173(2)	173(2)
θ range, degree	2.210 to 25.024	2.211 to 25.021
Reflections collected	42855	40964
Unique reflections	6790	6782
<i>R</i> _{int}	0.0425	0.0451
GOF on <i>F</i> ²	1.138	0.972
<i>R</i> ₁ /w <i>R</i> ₂ ^a (<i>I</i> > 2σ(<i>I</i>))	0.0842/0.2704	0.0754/0.2305
<i>R</i> ₁ /w <i>R</i> ₂ ^a (all data)	0.1165/0.3152	0.1323/0.2974
Flack parameter	0.23(4)	0.17(4)

^a $R_1 = \Sigma ||F_o| - |F_c|| / \Sigma |F_o|$, $wR_2 = [\sum w(F_o^2 - F_c^2)^2 / \sum w(F_o^2)]^{1/2}$

*The disordered guest molecules were calculated by the PLATON/SQUEEZE program combined with the charge conservation, elemental analyses and thermogravimetric analyses.

Table S2. Selected bond lengths (Å) and angles (°) for compounds **1P** and **1M**.

Bond lengths (Å)			
1P		1M	
Zn(1)-O(3)#1	1.951(8)	Zn(1)-O(3)	1.970(9)
Zn(1)-O(3)	1.951(8)	Zn(1)-O(3)#1	1.970(9)
Zn(1)-O(6)#2	1.991(9)	Zn(1)-O(6)#2	2.026(11)
Zn(1)-O(6)#3	1.991(9)	Zn(1)-O(6)#3	2.026(11)
Zn(2)-O(2)#4	1.953(9)	Zn(2)-O(2)#4	1.931(9)
Zn(2)-O(9)	1.979(4)	Zn(2)-O(9)	1.991(4)
Zn(2)-O(7)	1.997(10)	Zn(2)-O(1)	2.011(7)
Zn(2)-O(1)	2.007(7)	Zn(2)-O(7)	2.018(9)
Bond angles (°)			
1P		1M	
O(3)#1-Zn(1)-O(3)	107.4(5)	O(3)-Zn(1)-O(3)#1	110.5(5)
O(3)#1-Zn(1)-O(6)#2	104.4(5)	O(3)-Zn(1)-O(6)#2	102.3(5)
O(3)-Zn(1)-O(6)#2	120.0(4)	O(3)#1-Zn(1)-O(6)#2	119.1(4)
O(3)#1-Zn(1)-O(6)#3	120.0(4)	O(3)-Zn(1)-O(6)#3	119.1(4)
O(3)-Zn(1)-O(6)#3	104.4(5)	O(3)#1-Zn(1)-O(6)#3	102.3(5)
O(6)#2-Zn(1)-O(6)#3	101.6(6)	O(6)#2-Zn(1)-O(6)#3	104.4(7)
O(2)#4-Zn(2)-O(9)	110.7(3)	O(2)#4-Zn(2)-O(9)	109.5(3)
O(2)#4-Zn(2)-O(7)	118.5(4)	O(2)#4-Zn(2)-O(1)	97.5(4)
O(9)-Zn(2)-O(7)	123.2(3)	O(9)-Zn(2)-O(1)	106.5(4)
O(2)#4-Zn(2)-O(1)	96.2(4)	O(2)#4-Zn(2)-O(7)	118.5(4)
O(9)-Zn(2)-O(1)	105.1(4)	O(9)-Zn(2)-O(7)	123.5(3)
O(7)-Zn(2)-O(1)	96.3(4)	O(1)-Zn(2)-O(7)	95.4(4)

Symmetry transformations used to generate equivalent atoms:	Symmetry transformations used to generate equivalent atoms:
#1 -x+1,-y+1,z+0	#1 -x+2,-y+0,z+0
#2 -z+3/4,-y+5/4,-x+3/4	#2 x+1/4,-z+1/4,y+1/4
#3 z+1/4,y-1/4,-x+3/4	#3 -x+7/4,z-1/4,y+1/4
#4 -y+1,z+1/2,-x+1/2	#4 -z+1,-x+1,y+0

Table S3. A summary of structure determinations of six crystals randomly selected from six different reactors.

SN	a	R ₁	wR ₂	Flack parameter	Helicity
1	45.1476(7)	0.1165	0.3152	0.23(4)	1P
2	45.1661(6)	0.1221	0.3208	0.24(4)	1P
3	45.0262(9)	0.1932	0.3593	0.21(5)	1P
4	45.0572(13)	0.1687	0.3316	0.26(5)	1P
5	45.082(2)	0.1572	0.3106	0.30(4)	1P
6	45.1207(6)	0.1323	0.2974	0.17(4)	1M

Table S4. The ICP data.

Metal ion	The concentration of metal ion in the original DMF solution, mmol L ⁻¹	The concentration of metal ion in the DMF solution after adsorption, mmol L ⁻¹
Zn ²⁺	1.0500	0.9902
Ni ²⁺	1.0610	1.0204
Cd ²⁺	1.0394	1.0179
Na ⁺	0.9840	0.9187
Cu ²⁺	0.9749	0.9213
Cr ³⁺	0.9720	0.9153
Co ²⁺	0.9905	0.9248
Mg ²⁺	1.0338	0.9753
Mn ²⁺	1.0104	0.9428
Pb ²⁺	1.0158	0.9683
Fe ³⁺	0.9815	0.9468

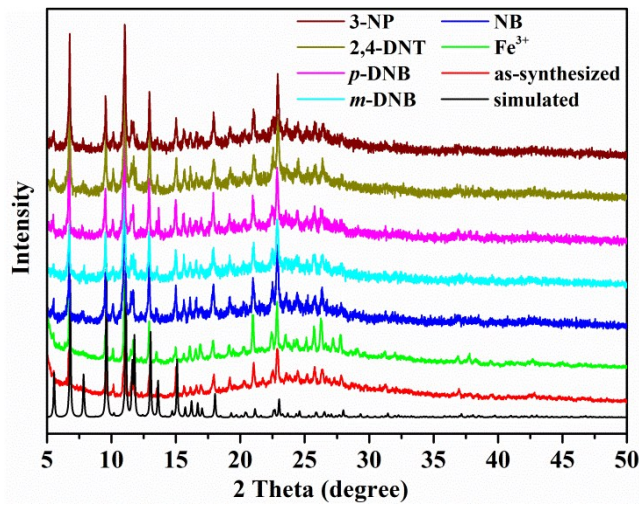


Figure S1. PXRD patterns of **1**: simulated, as-synthesized, soaked by DMF containing 50 mmol L⁻¹ nitro explosives (3-NP, 2,4-DNT, *p*-DNB, *m*-DNB, or NB), and soaked by DMF containing 1 mmol L⁻¹ Fe³⁺.

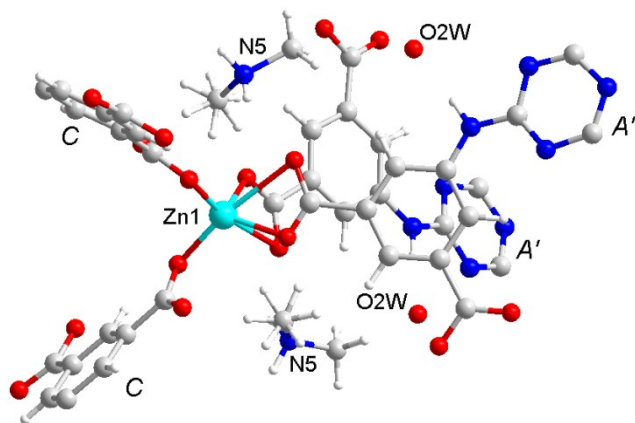


Figure S2. The location of one of the $[(\text{CH}_3)_2\text{NH}_2]^+$ cations in compound **1P**. *A'* and *C* are the conformations taken by the ligand. C gray, H white, N blue, O red, and Zn turquoise.

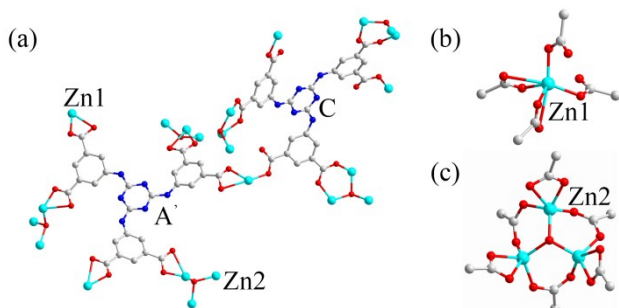


Figure S3. Coordination environments of TATAT⁶⁻ (a), Zn1 (b) and (Zn₃O) unit (c). C gray, N blue, O red Zn turquoise.

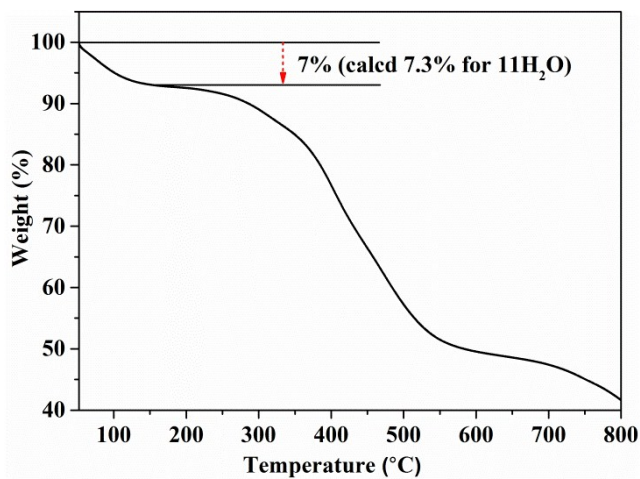


Figure S4. TGA curve of **1**.

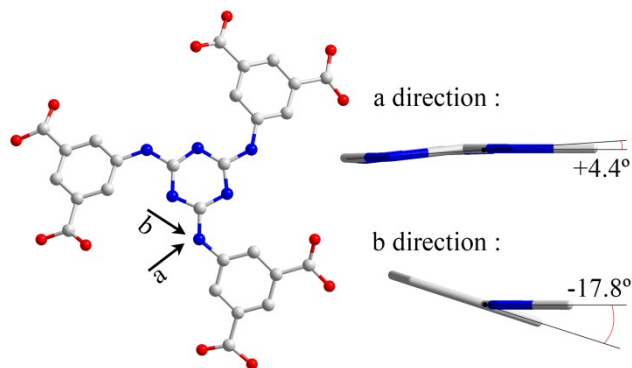


Figure S5. The dihedral angles formed by the C-NH-C plane with the benzene ring and the triazine ring in TATAT⁶⁻ ligand with conformation *C* of **1P**.

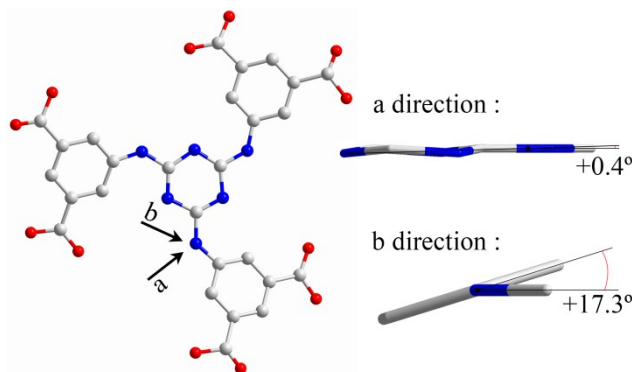


Figure S6. The dihedral angles formed by the C-NH-C plane with the benzene ring and the triazine ring in TATAT⁶⁻ ligand with conformation *A'* of **1P**.

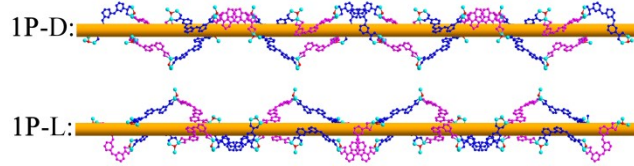


Figure S7. The arrangement of two non-mirrored conformations (A' and C) in helical channels **1P-D** and **1P-L** of **1P**. Conformations C blue, Conformations A' pink, O red and Zn turquoise.

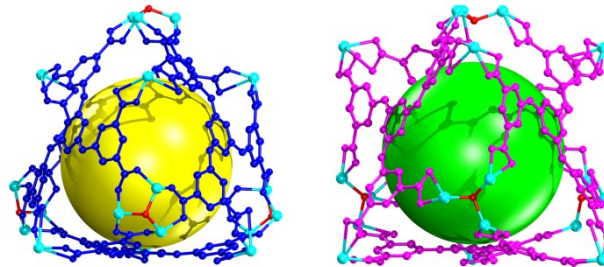


Figure S8. Two kinds of cages in **1P**. Conformations C blue, Conformations A' pink, O red and Zn turquoise.

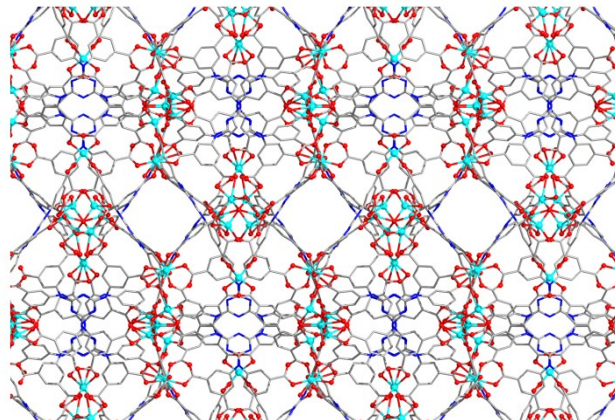


Figure S9. Distorted quadrilateral pores of **1P**, viewed along [1-10] direction. C gray, N blue, O red and Zn turquoise.

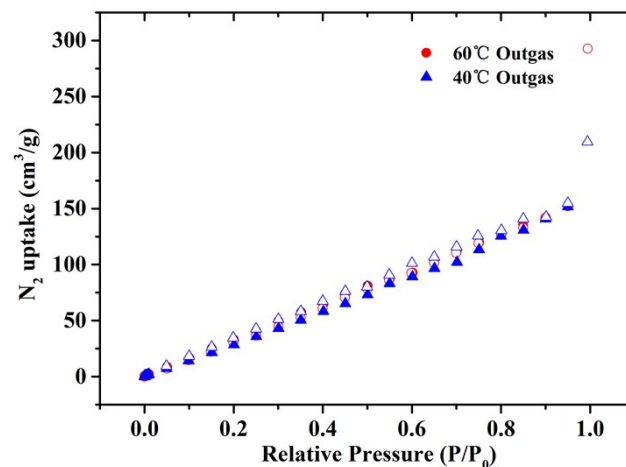


Figure S10. The N_2 sorption isotherm at 77 K (Filled symbols: adsorption, open symbols: desorption) for **1**.

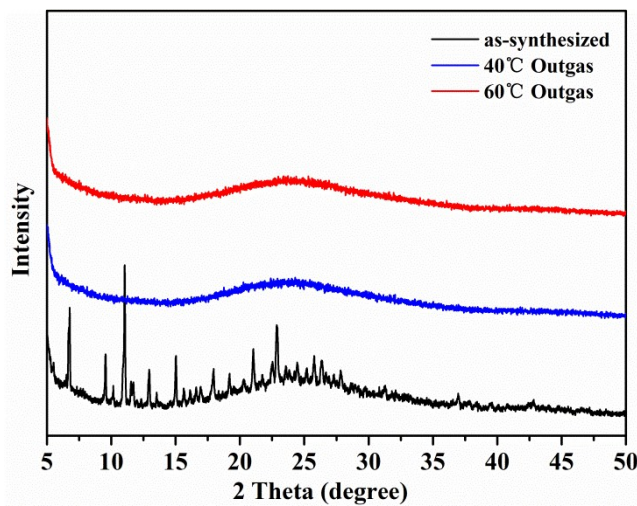


Figure S11. PXRD patterns of compound **1** after N_2 adsorption.

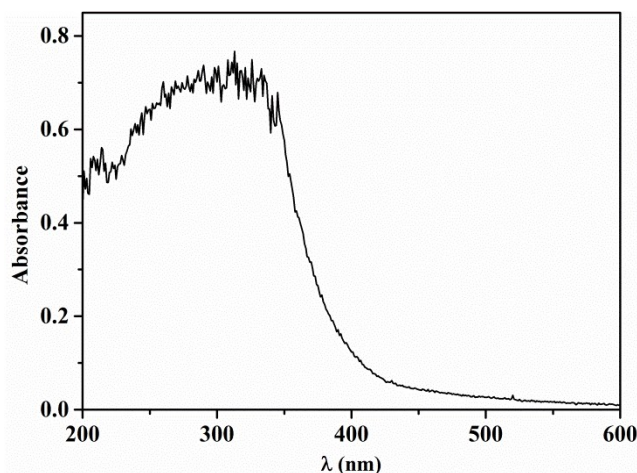


Figure S12. The UV-vis diffuse reflectance spectra of compound **1** in BaSO_4 plate.

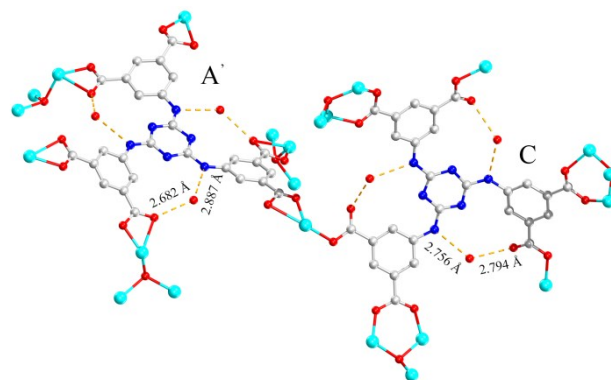


Figure S13. The hydrogen bond interactions between the TATAT^{6-} ligands and the water molecules in compound **1P**. C gray, N blue, O red and Zn turquoise.

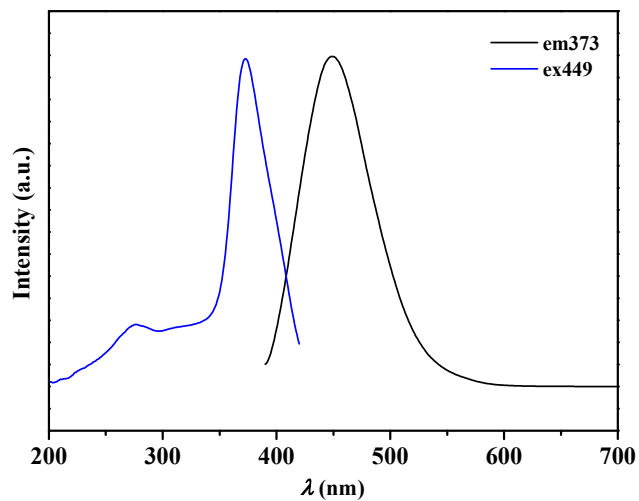


Figure S14. Excitation and emission spectra of compound **1** at room temperature.

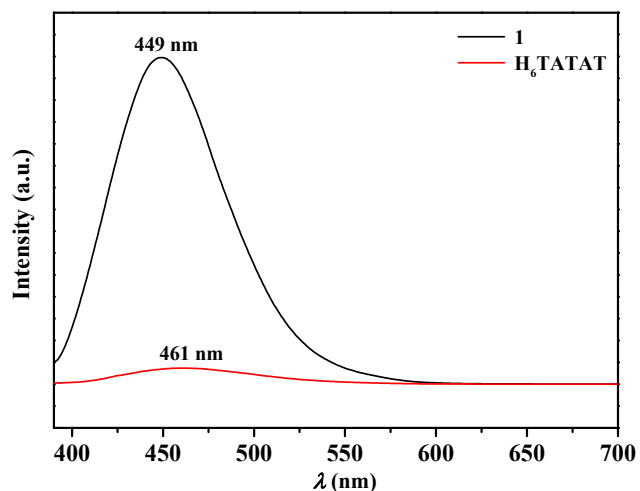


Figure S15. The solid photoluminescence spectra of compound **1** and H_6TATAT ligand excited at 373 nm.

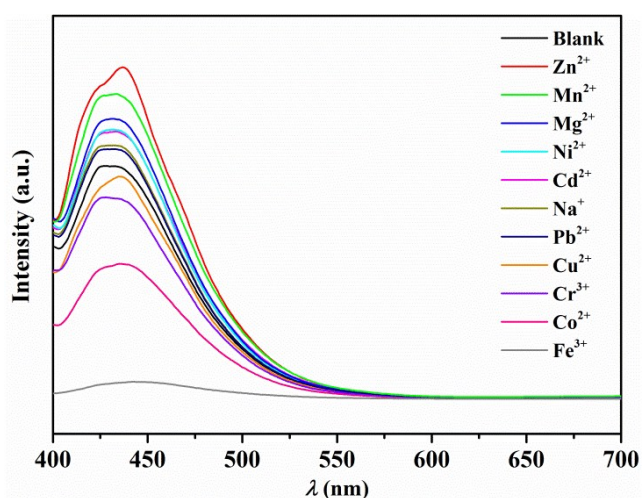


Figure S16. Luminescence spectra of **1** in DMF solutions with different cations (1 mmol L^{-1}).

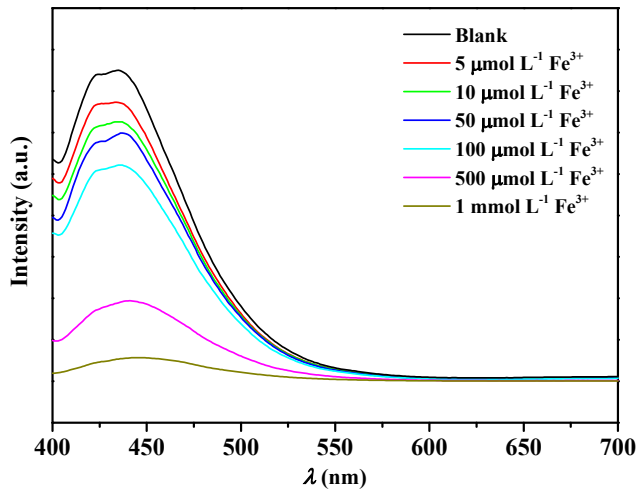


Figure S17. The luminescent spectra of **1** in DMF solutions with different concentrations of Fe^{3+} .

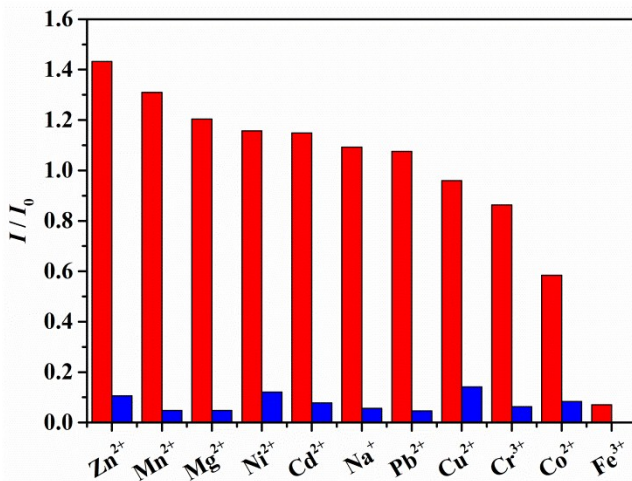


Figure S18. The antijamming experimental spectra of compound **1** on Fe^{3+} sensing (red bars, luminescent intensity of compound **1** with an ion; blue bars, luminescent intensity of compound **1** with an ion and Fe^{3+}).

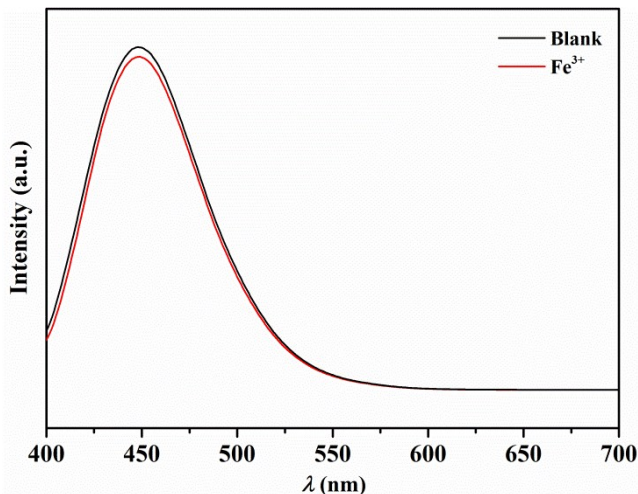
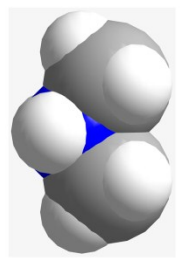


Figure S19. The solid fluorescent spectra of compound **1** after soaking in DMF solution and DMF solution of Fe^{3+} (1 mmol L^{-1}) for 1 day.



$4.0 \times 4.3 \times 6.4$ (Å)

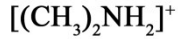


Figure S20. The dimensions of $[(\text{CH}_3)_2\text{NH}_2]^+$ cation.

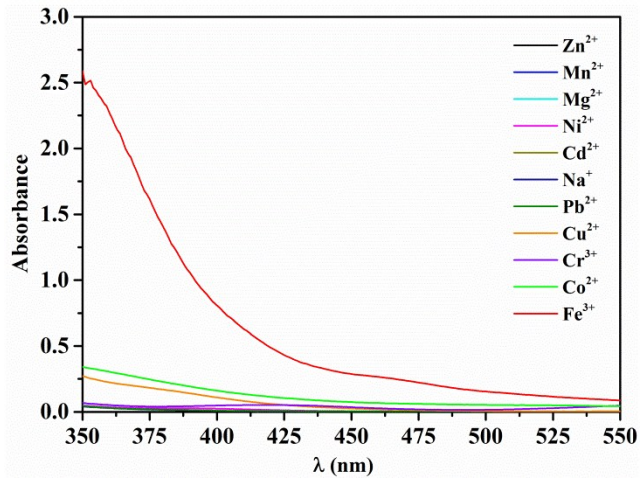


Figure S21. The absorbance spectra of metal ions in DMF (1 mmol L^{-1}).

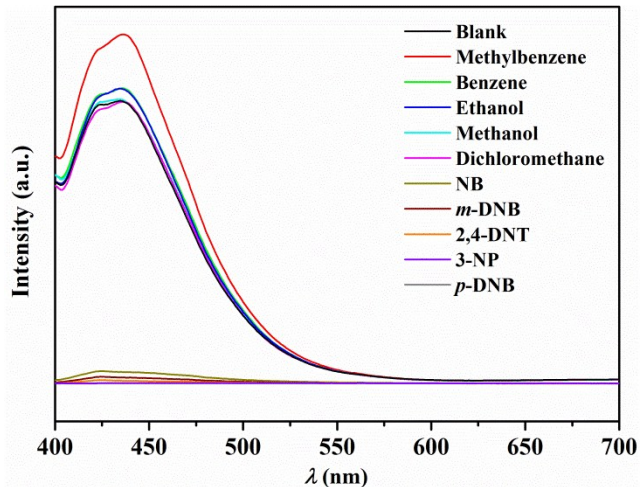


Figure S22. The luminescent spectra of **1** in DMF solutions containing different organic molecules (50 mmol L^{-1}) upon excitation at 373 nm .

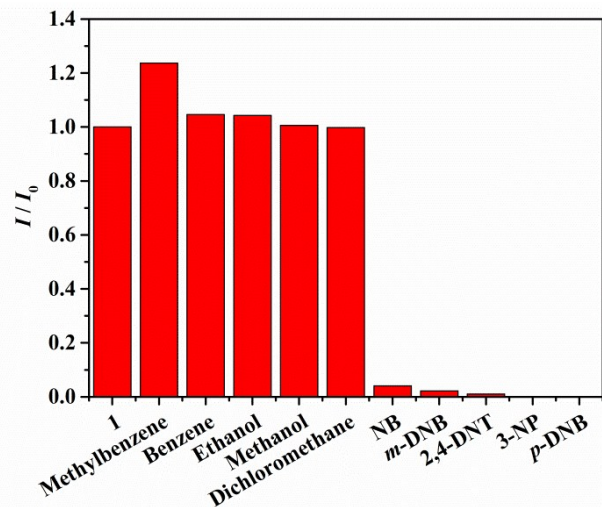


Figure S23. Luminescent intensity at 436 nm of the DMF suspension of **1** treated with 50 mmol L⁻¹ diverse nitro explosives.

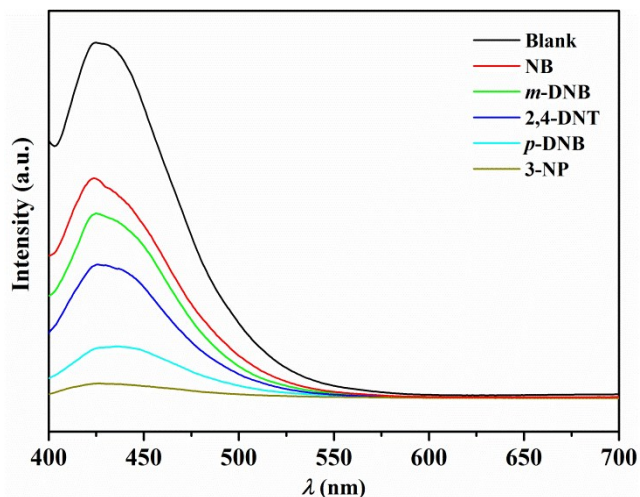


Figure S24. The luminescent spectra of **1** in DMF solutions containing different nitro explosives (5 mmol L⁻¹).

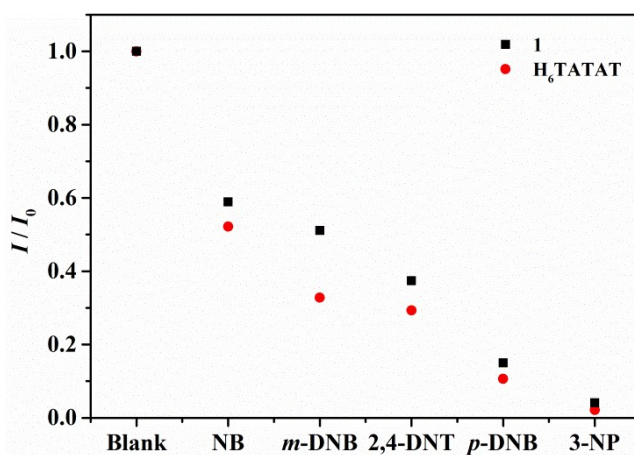


Figure S25. Luminescent intensity at 436 nm of the DMF suspension of **1** (0.18 mg mL⁻¹) and at 416 nm of the DMF solution of H_6TATAT (0.3 mg mL⁻¹) treated with 5 mmol L⁻¹ diverse nitro explosives upon excitation at 373 nm.

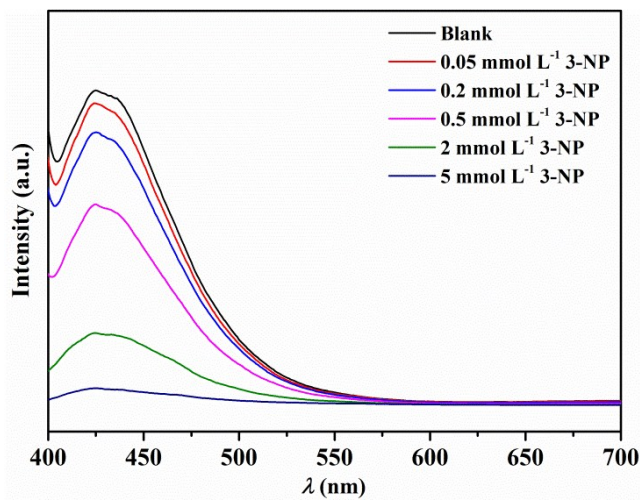


Figure S26. Emission spectra of **1** with addition of different concentrations of 3-NP in DMF solutions.

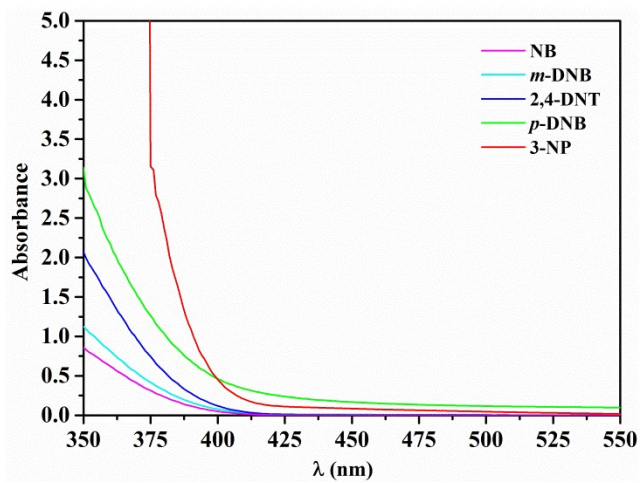


Figure S27. The absorbance spectra of nitro explosives in DMF (5 mmol L⁻¹).

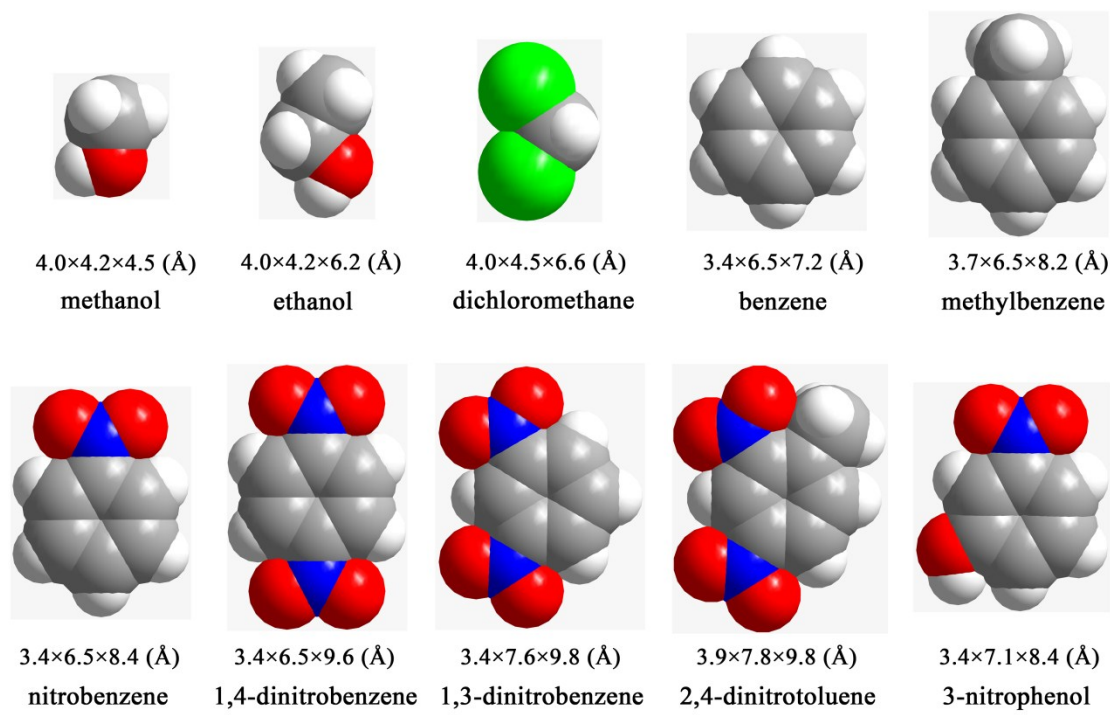


Figure S28. The dimensions of methanol, ethanol, dichloromethane, benzene, methylbenzene, nitrobenzene, 1,4-dinitrobenzene, 1,3-dinitrobenzene, 2,4-dinitrotoluene, and 3-nitrophenol.